

# Kinetics of low scattering biotissue photodenaturation induced by the UV harmonics of a Nd: YAP laser and by Nd: YAG laser at a wavelength of 1440nm

Nikita M. Bityurin\*, Sergey V. Muraviov, Vladislav A. Kamensky, Aleksey Yu. Malyshev, Evgeny V. Chelnokov, Lev V. Soustov, Grigory V. Gelikonov  
Institute of Applied Physics, RAS, 603600, Nizhnii Novgorod, Russia

## ABSTRACT

We study the effect of laser radiation on initially low scattering media such as egg white and crystalline substance. These media become highly scattering under laser irradiation. We perform and discuss three kinds of experiments, which elucidate the time dynamics of scattering of probe radiation. In the experiment of the first kind we investigate the pure photothermal denaturation of tissues under the effect of a Nd:YAG laser at a wavelength of 1440nm (absorption coefficient in water is  $26\text{cm}^{-1}$ ). The theoretical model is derived which enables us to estimate the temperature rise involved. It also allows us to estimate the corresponding kinetics parameters of photodenaturation and characteristics of probe light scattering. In the experiment of the second kind we perform multiple pulse irradiation of tissues by UV harmonics (the fourth and the fifth) of a Nd:YAP laser with the aim to determine the characteristics of pure photochemical modification of materials. In these experiments the fluences were small enough to prevent heating of the materials. The results of the above experiments both of the first and the second kind allow us to estimate the relative contributions of photochemical modification of a tissue and photothermal protein denaturation within the experiments of the third kind, in which we use the mentioned above UV solid state laser harmonics at fluences high enough to produce heating of the materials.

**Keywords:** biological tissue, denaturation, IR laser, UV laser, photothermal, photochemical

## 1. INTRODUCTION

The elucidation of the main features of laser-induced denaturation of biological tissues provides necessary information for employing different kinds of lasers for biomedical applications<sup>1</sup>. Recently, experimental data on kinetics of photodenaturation of soft biological tissues by means of CTH:YAG (holmium laser) and CO<sub>2</sub> lasers were reported<sup>2,4</sup>. In the present communication we investigate photodenaturation of several tissues, which was induced by a Nd:YAG laser tuned to a wavelength 1440 nm (absorption coefficient in water is  $26\text{cm}^{-1}$ ) and the UV harmonics of a Nd:YAP laser ( $\lambda=270\text{nm}$ ,  $\lambda=216\text{nm}$ ). It is of interest to compare kinetics of photodenaturation of the same tissue at different wavelengths and to verify the possibility of describing this process by relatively simple models.

## 2. MATERIALS AND METHODS

We investigate the effect of laser radiation on egg white and crystalline substance. The latter was extracted from the porcine eye obtained from a local slaughterhouse. The eyes were kept in refrigerator and were used within 24 hours after death. The specially designed cell was filled by the raw egg white or raw crystalline substance. This cell consists of front and rare fused silica windows lodged inside a metal cylindrical framing. The thickness of the investigated media between the windows was regulated by a Teflon spacer and ranged from 50 to 1000 $\mu\text{m}$ . The diameter of the sample was 3 cm, the thickness of the windows being 0.6 cm. Both egg white and crystalline substance are initially transparent media demonstrating significant changes in light transmittance under the effect of laser radiation mainly due to induced scattering. The typical experimental setup for investigating dynamics and kinetics of induced scattering is shown in Fig.1. As a source of irradiating laser beam we used a self-made free-running Nd:YAG laser tuned to a wavelength of 1440 nm (absorption coefficient in water is  $26\text{cm}^{-1}$ ) and the UV harmonics of a self-made Q-switched Nd:YAP laser ( $\lambda=270\text{nm}$ ,  $\lambda=216\text{nm}$ ). A XeCl excimer laser ( $\lambda=308\text{nm}$ ) (Lambda Physics LPX200) was also employed as a source of UV radiation. We perform two types of experiments. In the experiments of a first kind we investigate time-resolved dynamics of photothermal denaturation of

\* Correspondence: E-mail: [bit@appl.sci-nnov.ru](mailto:bit@appl.sci-nnov.ru); Telephone: +7-8312-384389; FAX: +7-8312-363792

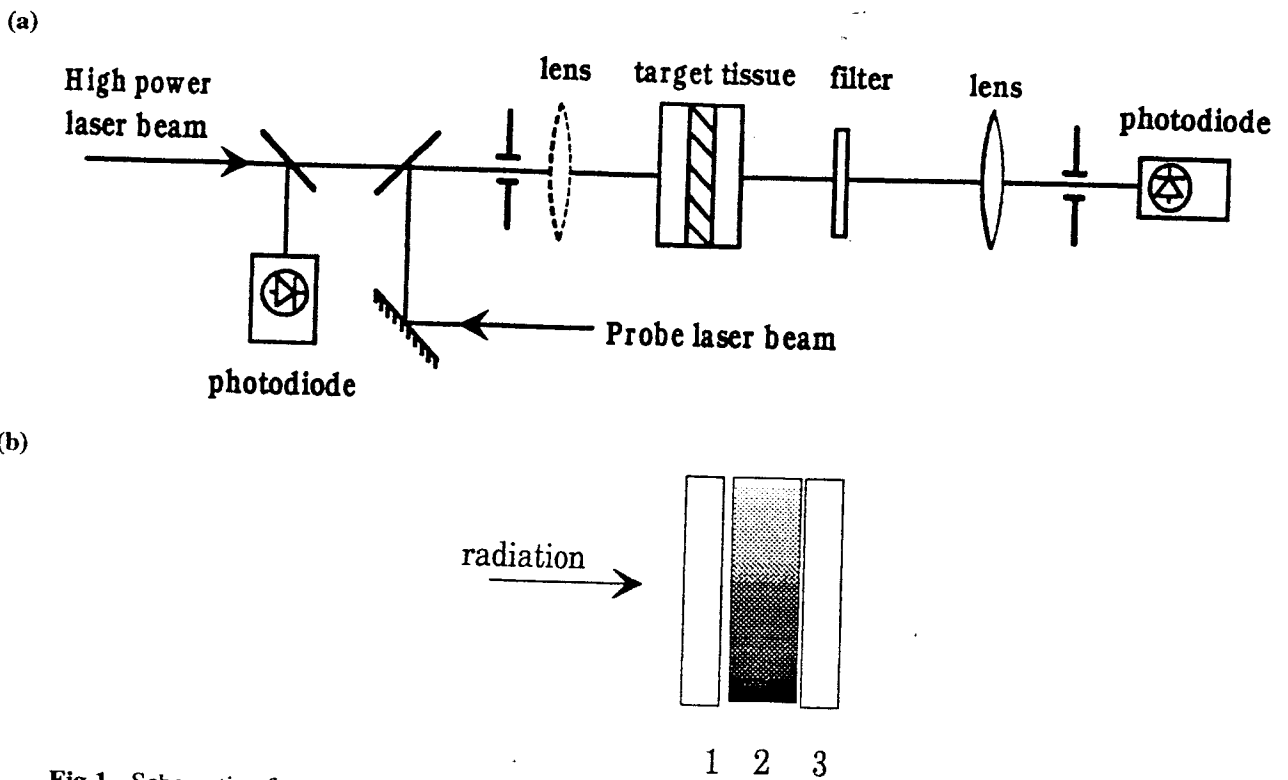


Fig.1. Schematic of measurements of scattering associated with photodenaturation of transparent protein media (a). Schematic of the cell containing a biological medium (b).

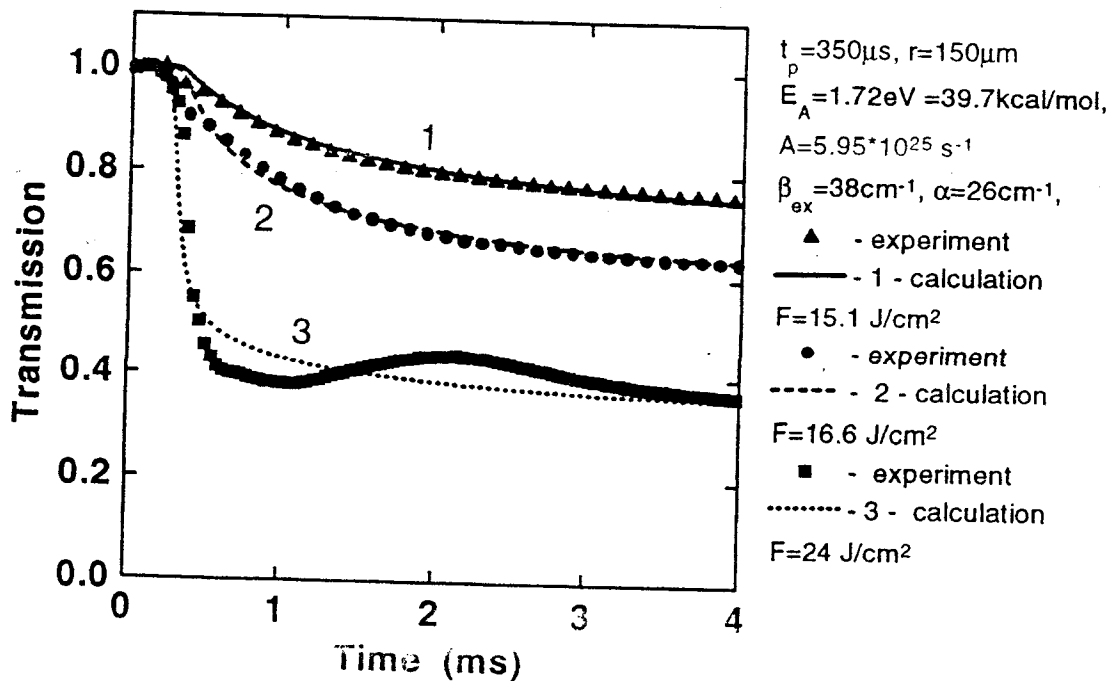


Fig.2. Oscillogram of probe radiation passing through a scattering area that occurs after irradiation of egg white at  $\lambda = 1.44 \mu\text{m}$ . The cell consists of two IR quartz plates. The thickness of the medium is 1 mm. High power laser pulse duration is 350  $\mu\text{s}$ .

tissue. Here free-running Nd:YAG laser radiation at a wavelength of 1.44  $\mu\text{m}$  with pulse duration of 350  $\mu\text{s}$  was used as a source of high power radiation and a single-mode highly stable cw laser radiation at a wavelength of 0.83  $\mu\text{m}$  was used as a probe. Two processes occurred in the irradiation area: photothermal denaturation of protein and a thermal lens formation. The both processes are accompanied by increased scattering evidenced by changes in transmitted power of probe cw laser radiation through diaphragm in the image plane. The photodenaturation leads to scattering at wider angles than the thermal lens. Thus, changes in the laser beam divergence due to the thermal lens formed in the material can be accounted for by the size of the diaphragm in the image plane. In the experiments of the second kind we follow pulse to pulse kinetics of light scattering induced by the irradiation of tissue by UV harmonics of a Q-switched Nd:YAP laser with pulse duration 10ns (the fourth,  $\lambda=270\text{nm}$ , and the fifth,  $\lambda=216\text{nm}$ ). We investigated both photochemical modification of tissue by laser pulses of relatively small fluences, when heating was negligible, and modification by laser pulses with higher fluences when heating was significant. The temperature is estimated using the model discussed below. In the experiments of this kind we employ a He-Ne laser ( $\lambda=632.8\text{nm}$ ) as a probe, receiving diaphragm placed at the focus plane of the lens. The dimension of the diaphragm can be chosen from consideration of initial divergence of the probe beam.

### 3. THE MODEL

The model includes the heat diffusion equations

$$\frac{\partial T}{\partial t} = D_T^i \frac{\partial^2 T}{\partial z^2} + \frac{\alpha^i I}{c_p^i \rho^i} - D_T^i \frac{B}{r_B^2} \quad (1)$$

denaturation-kinetics equation

$$\frac{\partial N}{\partial t} = A(1 - N) \exp(-E_A/RT) \quad (2)$$

and light propagation equations for actuating radiation and a probe beam.

$$\frac{\partial I}{\partial z} = -\alpha I \quad (3)$$

$$\frac{\partial I_{probe}}{\partial z} = -\beta_{ex} N I_{probe} \quad (4)$$

Here  $D^i$ ,  $\alpha^i$ ,  $c_p^i$ ,  $\rho^i$  for  $i=1,2,3$  are thermal diffusivity, absorption coefficient at irradiating wavelength, specific heat, and density of biotissue and material of the windows, respectively. Here the superscript 1 refers to the front window, 2 - to the biological media, 3 - to the rare window. Boundary conditions are the continuous heat flux between biotissue and windows.  $N(z,t)$  is the fraction of coagulated material along the optical axis  $z$  at moment  $t$ .  $I$ ,  $I_{probe}$  are intensities of irradiating pulse and probe radiation, respectively.  $\beta_{ex}$  refers to the extinction coefficient.  $R$  is the gas constant.  $z=0$  corresponds to the boundary of the biological medium.

We suppose that extinction of a probe beam is connected with scattering on photocoagulated components. At the same time, for actuating radiation it is supposed that the appearing scattering does not affect a temperature distribution in biotissue, which is determined mainly by absorption. A significant denaturation occurs after a power laser pulse.

The model (1) - (4) is used to describe the experiments performed by us and discussed in this communication. The model (1) - (3) can be also applied to the experiments of Ref. 3. Here the role of face windows 1 is played by a fiber delivering the laser radiation and the rare window 2 is absent. The model is essentially one-dimensional. The radial heat flux in cylindrical geometry is accounted for by the last term in (1). Here  $r_B$  stands for the beam radius,  $B$  being the constant equal to 3.56 for a Gaussian beam. Solving the above sets of partial differential equations we use numerical calculations. These calculations follow the approaches considered in<sup>5</sup> to finite difference methods of solving linear parabolic differential equations. We used

implicit schemes accompanied by sweeping method of solving corresponding sets of linear algebraic equations. The most important point is the use of variable coordinate steps. The distribution of steps should take into account the different space scales involved: Bueger scale and heat diffusion scales regarding pulse duration and time of observation. The similar approach has been used by us when modeling UV laser ablation of polymers (for review see <sup>6</sup>) and correlates with approach <sup>7</sup>.

## 4. RESULTS AND DISCUSSIONS

### 4.1. IR photothermal denaturation

Using the above model, we compared the numerical modeling of photodenaturation of egg white with experimental data from paper<sup>3</sup> where an observation of growth of coagulated zone under holmium laser radiation by a fast CCD camera was reported. Figure 3 shows the calculated position of the domain of denaturation. Here  $z=0$  corresponds to the boundary of the fiber through which the laser light was delivered into the egg white. It is seen that the correspondence is good enough. These theoretical curves are calculated using the following kinetic parameters: activation energy is  $E_A=39.7$  kcal/mol with pre-exponential factor  $A=5.95 \cdot 10^{25} \text{ s}^{-1}$ . This is higher than in paper<sup>2</sup> for photodenaturation of muscular tissues by a  $\text{CO}_2$  laser ( $E_A=12.1$  kcal/mol and  $A=6.5 \cdot 10^7 \text{ s}^{-1}$ ), but smaller than for usual slow heating of egg white ( $E_A=83$  kcal/mol and  $A=1.3 \cdot 10^{52} \text{ s}^{-1}$ ).

In our experiments, denaturation kinetics was registered by scattering of probe radiation. That is why for comparison with obtained experimental results it was necessary to make numerical computations of transmission of a probe beam through the coagulated medium by choosing appropriate extinction coefficient  $\beta_{ex}$  when other parameters of the model were fixed. In computations we used values  $E_A$ ,  $A$  which we determined earlier for egg white. As a result, the extinction coefficient was found to be  $\beta_{ex} = 38 \text{ cm}^{-1}$ . Comparing experimental and theoretical curves, one can note that the theoretical modeling is in quite good accord with experiment (Fig. 2, curves 1 and 2). Numerical computation showed that the time of formation of a scattering layer is determined by the time of thermal wave propagation along the cell.

At an increased energy density we obtained oscillograms (Curve 3 in Fig.2) in which, along with denaturation, bubbles of water vapor are formed inside biotissue. For a holmium laser the threshold of bubbles formation was reported<sup>3</sup> to be  $32 \pm 5 \text{ J/cm}^2$  at a pulse duration of  $130 \mu\text{s}$  and  $40 \pm 5 \text{ J/cm}^2$  at a pulse duration of  $1000 \mu\text{s}$ . In our experiments we have the threshold near  $30 \text{ J/cm}^2$  at the wavelength of  $1.44 \mu\text{m}$ . It should be noted that absorption coefficient of water at the wavelength of a holmium laser and at the wavelength  $1.44 \mu\text{m}$  are close to each other. Fig.4 exhibits the temperature distribution just after the pulse inside the egg white near the fiber boundary. These distributions correspond to the threshold fluence for bubble formation reported in Ref. 3 for different pulse duration. It is seen that the maximum values of temperature are different whereas the boundary values are much closer to each other. From the theory of phase transitions of the first order it is known that boundaries are the most probable sites for bubble creation. Thus, we can connect the threshold of bubble formation with the temperature rise up to  $100^\circ \text{C}$  in the vicinity of the boundary. Fig.4 illustrates this statement.

### 4.2. UV photochemical modification

In our experiments on UV photochemical modification of biological tissues we perform multiple pulse irradiation of the above materials at small fluences. The maximum temperature here was significantly smaller than the denaturation temperature. It is known<sup>8</sup> that the UV irradiation of protein materials provides chain scission at relatively short wavelengths and protein aggregations at relatively long wavelengths ( $\lambda > 300 \text{ nm}$ ). Transmission spectra obtained just before and after irradiation show that the irradiation at wavelengths of  $270 \text{ nm}$  and  $216 \text{ nm}$  results in an increase in optical density at all wavelengths in UV and visible regions. The main effect is induced scattering except the region near  $\lambda=255 \text{ nm}$ . Fig.5 shows the dependence of transmission of probe laser beam on the integrated dose for different pulse fluences. Irradiation with different fluences was performed by the fifth harmonic of Nd:YAP laser ( $\lambda=216 \text{ nm}$ ), whereas probing was provided by the fourth harmonic of the same laser. It is seen that tissue response was almost reciprocal, i.e. the transmission of the probe depends on the dose independent of the pulse fluence. Fig.6 shows the response of the crystalline substance irradiated with the wavelength  $270 \text{ nm}$ . It is seen that this response is also almost reciprocal within the error of measurements. On the other hand we cannot say about reciprocity when the egg white is irradiated with the wavelength of  $270 \text{ nm}$  as it is shown in Fig.7

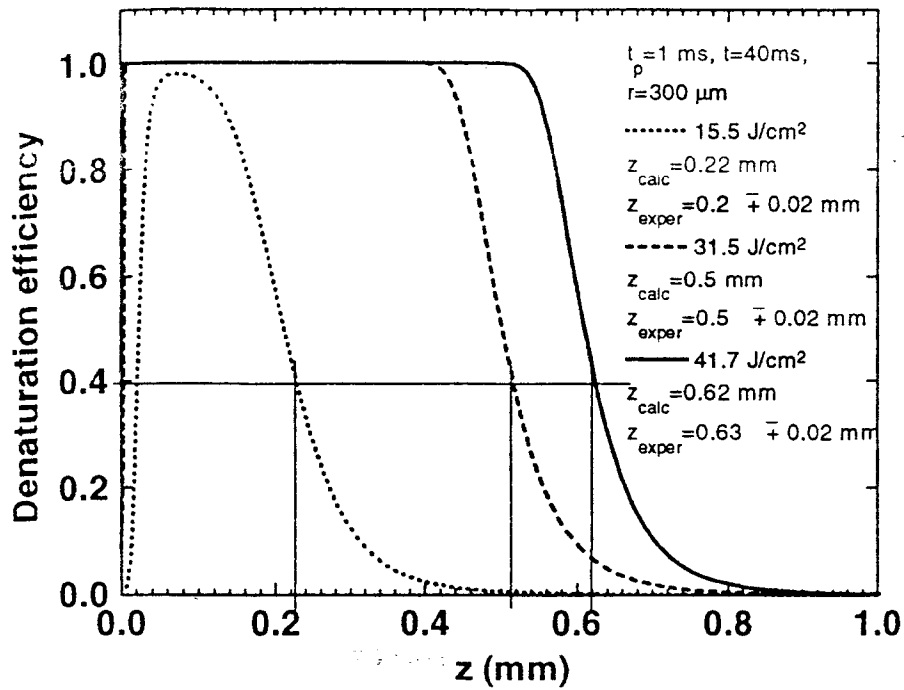


Fig.3. Calculated position of coagulated zone in egg white compared to the experimental data of Ref. 3. Irradiation was performed through the fiber.

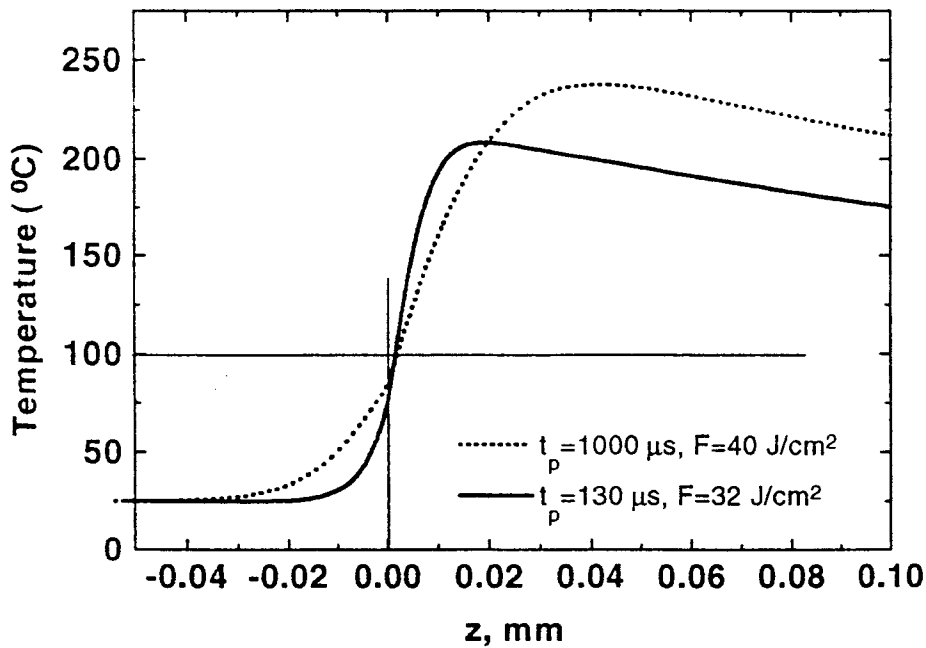


Fig.4. Calculated temperature distribution within the egg white corresponding to the threshold conditions for bubble creation for different pulse durations,  $t_p$ , according to the experimental data reported in Ref. 3.

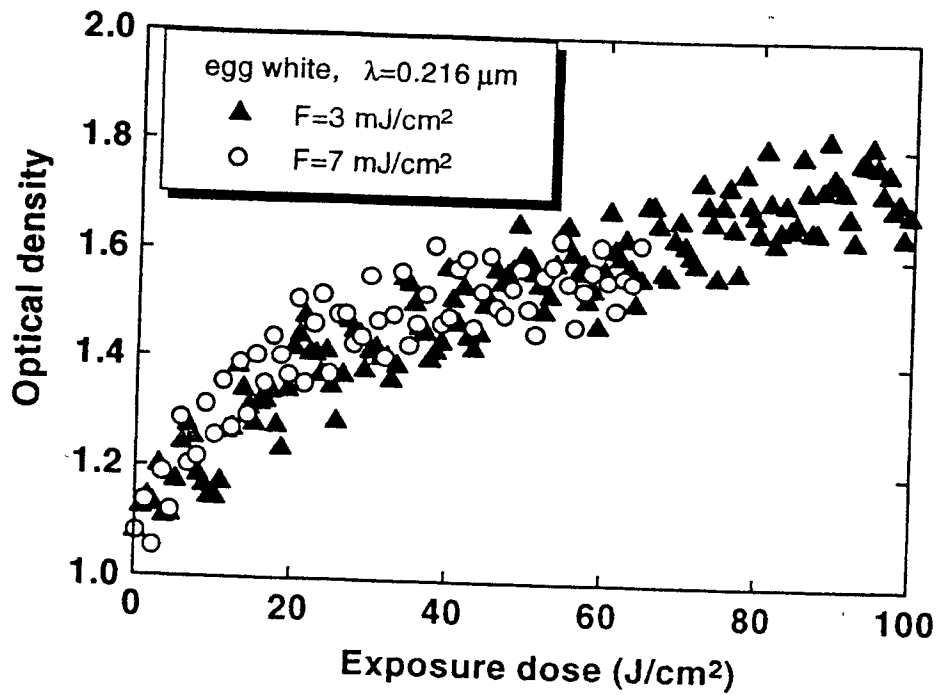


Fig.5. Optical density at the wavelength of probe radiation ( $\lambda=270\text{nm}$ ) as a function of exposure dose for different pulse fluences. Irradiation was performed at a wavelength of 216nm. The thickness of the medium ( egg white) is  $50 \mu\text{m}$ .

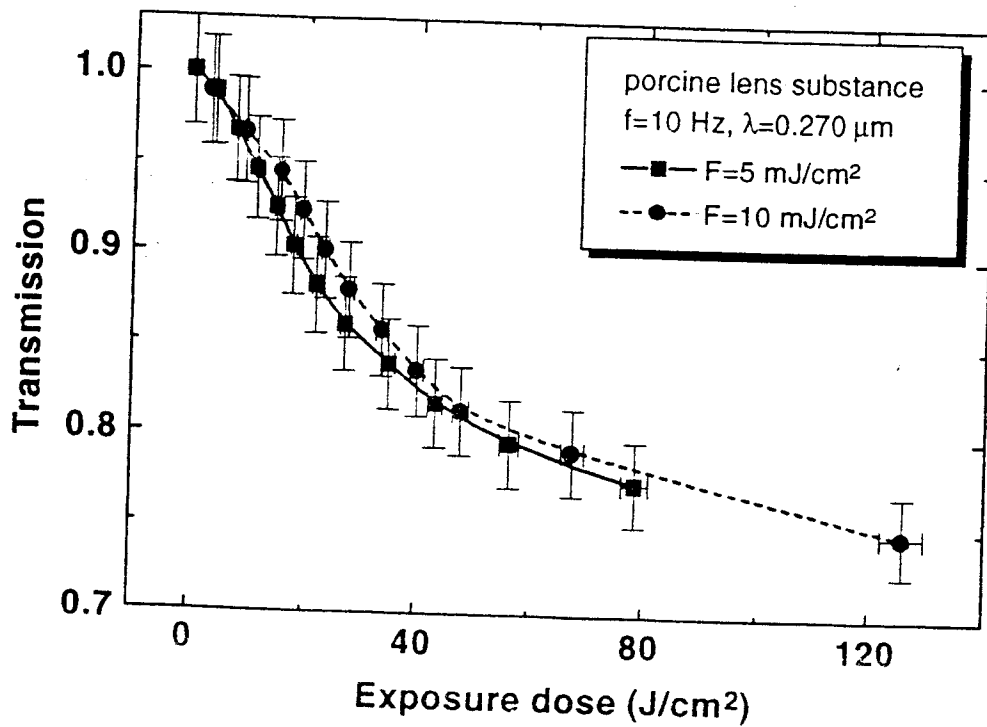


Fig.6. Transmission of the probe beam of He - Ne laser as a function of the exposure dose for different pulse fluences. Irradiation was performed at a wavelength of 270nm. The thickness of the medium ( porcine crystalline substance) is  $100 \mu\text{m}$ .

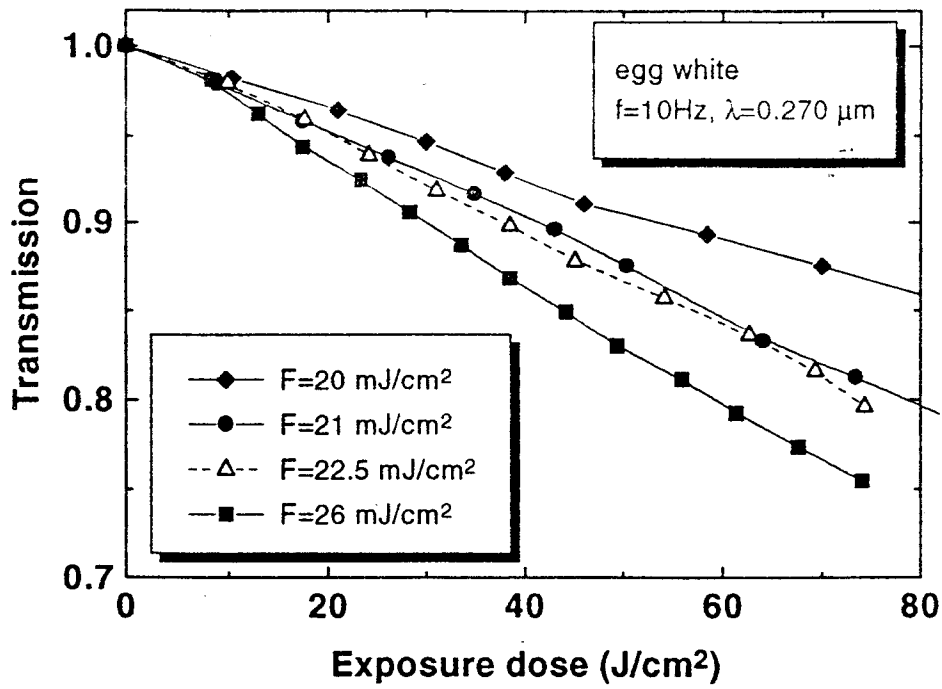


Fig.7. Transmission of the probe beam of He - Ne laser as a function of the exposure dose for different pulse fluences. Irradiation was performed at a wavelength of 270nm. The thickness of the medium ( egg white) is 100  $\mu\text{m}$ .

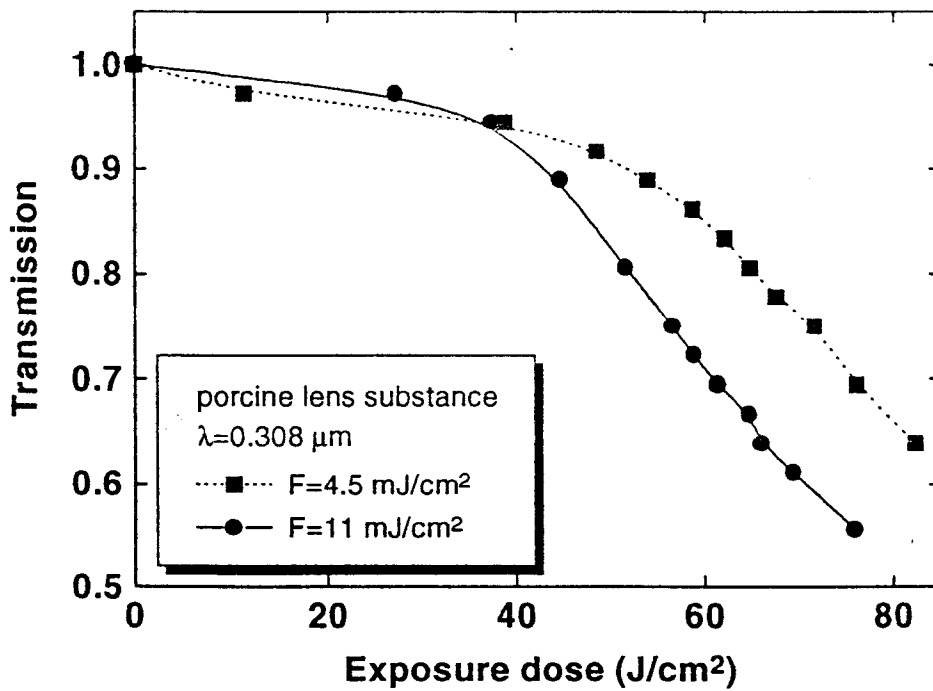


Fig.8. Transmission of the probe beam of He - Ne laser as a function of the exposure dose for different pulse fluences. Irradiation was performed at a wavelength of 308nm. The thickness of the medium ( porcine crystalline substance) is 100  $\mu\text{m}$ .

For comparison, we show (see Fig.8) the kinetics of the increase in scattering induced in porcine crystalline substance by the irradiation by a XeCl laser at a wavelength of 308nm. It is well known<sup>8</sup> that here protein aggregation dominates the modification process. Here we also observed nonreciprocal response as it is seen in Fig.8. While direct chain scission should not depend on pulse fluence but rather on an integrated dose, the aggregation where several macromolecules are involved in the process, can exhibit the nonreciprocal response. Thus, we can suppose that nonreciprocity at the wavelength of 270nm is also connected with aggregation, which occurs simultaneously with chain scission. Of course, this statement should be investigated in more detail but it is beyond the scope of the present communication. It is important for us now that the detectable change in transmittance of a probe beam owing to the photochemical modification occurs at the irradiation doses of the order of  $10\text{J}/\text{cm}^2$ .

#### 4.3. UV photothermal denaturation

Fig. 9 shows the temperature distribution and denaturation efficiency ( $N$ ) calculated according to the above pure photothermal model for a single pulse of the fourth harmonic for different fluences. It is seen that detectable denaturation starts at fluences about  $2\text{J}/\text{cm}^2$ . It follows from the above consideration that at these fluences the photochemical effect can be neglected and single pulse UV denaturation is purely photothermal. Of course, this statement can be invalid if there occurs dark thermally activated reaction, which can be initiated photochemically. A well known example of such kind is depolymerization, or unzipping, which takes place during thermal destruction of such additional polymers as Polymethylmethacrylate and can be significantly accelerated photochemically. Our experiments show that at fluence  $1\text{J}/\text{cm}^2$  egg white irradiated by a single pulse of the fourth harmonic did not show any detectable change in transmittance of a probe He-Ne beam while these changes occur at fluences about  $2\text{J}/\text{cm}^2$ . The microscope image of irradiated area exhibits the domain of thermal denaturation. It is in accordance with the purely photothermal model of single pulse denaturation. The problem with observation of this UV photothermal denaturation follows from the fact that the threshold of bubble formation is quite close to the threshold of denaturation. It is seen in Fig. 9 that the maximal value of temperature is somewhat higher than  $100^\circ\text{C}$  and this maximum appeared to be quite close to the window surface. The latter is connected with the value of absorption coefficient,  $\alpha=172\text{cm}^{-1}$  for egg white, (compare with  $26\text{cm}^{-1}$  at  $\lambda=1.44\mu\text{m}$ ) and with short, 10ns, pulse duration. This makes the probability of bubble formation high enough. This effect is even more pronounced with the fifth harmonic with the absorption coefficient in egg white of about  $5000\text{cm}^{-1}$ . During our experiments we were not able to obtain stable (without bubbles) photothermal single pulse denaturation of egg white by the fifth harmonic radiation. With the fourth harmonic beam we observed a regime of smooth single pulse denaturation of egg white almost without bubbles (see Fig.10), while most of our attempts resulted in bubble formation accompanied by the photothermal denaturation.

### 5. CONCLUSIONS

We considered the effect of IR and UV laser radiation on initially transparent (in the visible region) protein media such as raw egg white and raw porcine crystalline substance.

Our time resolved experiments on IR laser photothermal denaturation along with the data on IR laser denaturation kinetics reported in Ref.3 could be described by a simple photothermal model.

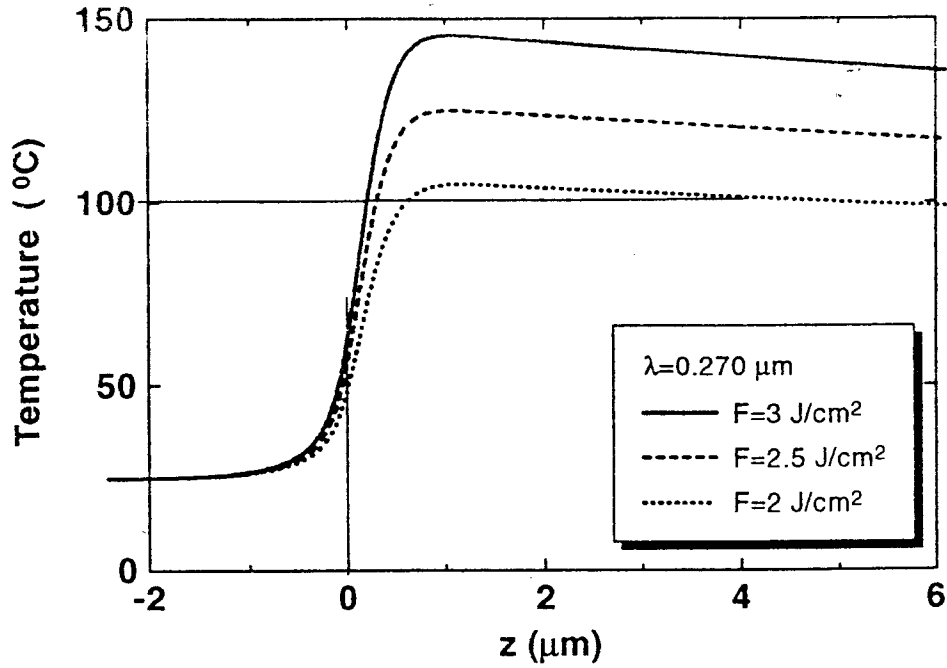
Multiple pulse irradiation of above tissues by UV lasers at fluences small enough to prevent heating demonstrates photochemical modifications of materials. The photochemical response can be reciprocal or nonreciprocal.

The features of single UV pulse modification of egg white at 270 nm (fourth harmonic of Nd:YAP laser) with fluences about  $2\text{J}/\text{cm}^2$  are in accordance with the purely photothermal model of denaturation considered above for IR irradiation. The threshold of bubble formation is very close to the threshold of photothermal denaturation.

### ACKNOWLEDGEMENTS

This work was supported by Russian Foundation for Basic Research (grant 00-02-16411).

(a)



(b)

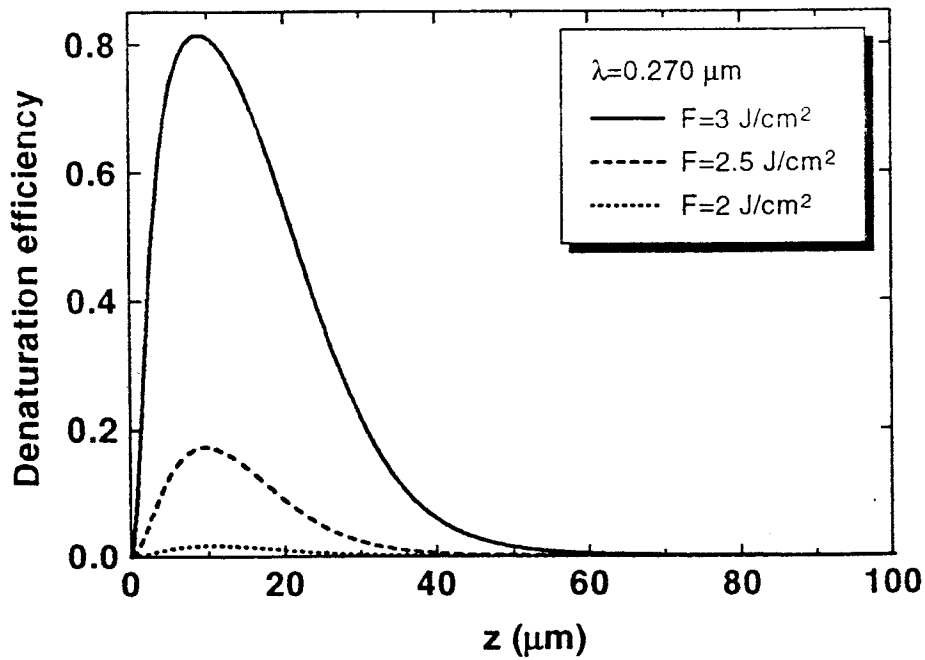
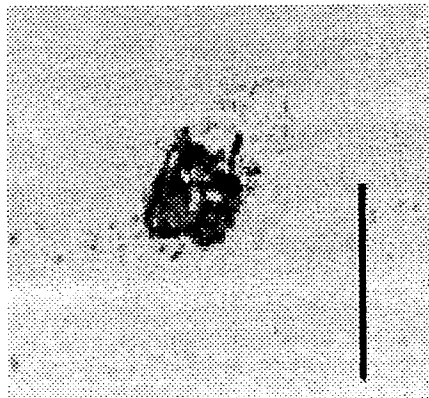


Fig.9. Calculated temperature distribution (a) in a cell with egg white in 250ns after irradiation by a single pulse of the fourth harmonic of a YAP:Nd laser ( $\lambda=270\text{nm}$ ) and resulting distribution of thermally coagulated component (b) for different pulse fluences.

(a)



(b)

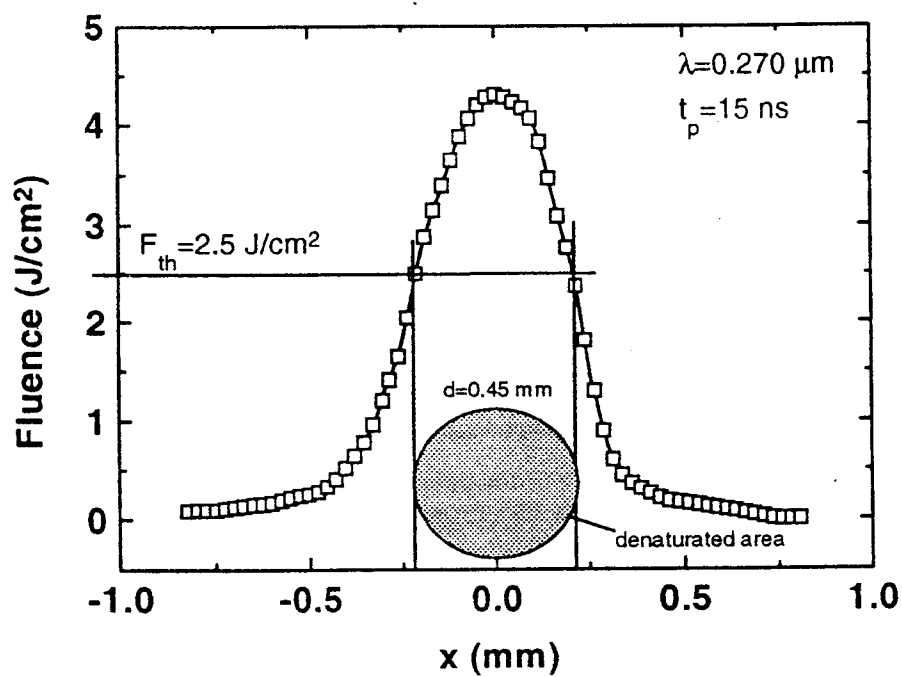


Fig.10. Photo image of the coagulated area produced by a single pulse of the fourth harmonic of a YAP:Nd laser ( $\lambda=270\text{nm}$ ) (a) and distribution of fluences in irradiated area (b).

## REFERENCES

1. A.J. Welsh, "The Thermal Response of Laser Irradiated Tissue", *IEEE Journal of Quantum Electronics*, 20, pp. 1471-1481, 1984.
2. V. Sankaran and J.T. Walsh, "An Optical, Real-time Measurement of Collagen Denaturation", *Proc. SPIE*, 2975, pp. 34-42, 1997.
3. T. Asshauer, G. Delacretaz, S. Rastegar, "Photothermal Denaturation of Egg White by Pulsed Holmium Laser", *Proc. SPIE*, 2681, pp. 120-124, 1996.
4. G. Huettmann, R. Birngruber, "Dynamics of thermal microeffects: rate constants of thermal denaturation measured by a temperature-jump experiment", Technical Digest of Conference *Therapeutic Laser Application*, pp 44-46, Orlando, 1998.
5. A.A. Samarskii, P.N. Vabishchevich, *Computational heat transfer*, John Wiley & Sons, New York, 1995.
6. N. Arnold, N. Bityurin, "Model for laser - induced thermal degradation and ablation of polymers", *Appl. Phys. A.*, 68, pp. 615-625, 1999.
7. R.A. London, M.E. Glinsky, G.B. Zimmerman, D.S. Bailey, D.C. Eder, and S.L. Jacques, "Laser-tissue interaction modeling with LATIS", *Appl. Optics*, 36, pp. 9068-9074, 1997.
8. R.F. Borkman, G. Knight, and B. Obi, "The Molecular Chaperone  $\alpha$ -Crystallin Inhibits UV - Induced Protein Aggregation", *Exp. Eye Res.*, 62, pp. 141-148, 1996